Faculty of Chemistry and Chemical Engineering
Babeș-Bolyai University
Cluj-Napoca, 400028
ROMANIA

BIOCHEMICALLY RELEVANT HETEROCYCLES AND COORDINATIVE COMPOUNDS

Summary

Mihai Surducan

Scientific advisors:

Prof. Dr. Luminita Silaghi-Dumitrescu, Faculty of Chemistry and Chemical Engineering, "Babeș-Bolyai" University, Cluj Napoca

Prof. Dr. Valentin Zaharia, Faculty of Pharmacy, "Iuliu Haţieganu" University of Medicine and Pharmacy, Cluj Napoca

Cluj-Napoca
2012

JURY

PRESIDENT

Conf. Dr. Luminița David, Faculty of Chemistry and Chemical Engineering, Babeș-Bolyai University, Cluj-Napoca, Romania.

SCIENTIFIC ADVISORS:

Prof. Dr. Luminita Silaghi-Dumitrescu, Faculty of Chemistry and Chemical Engineering, "Babeș-Bolyai" University, Cluj Napoca

Prof. Dr. Valentin Zaharia, Faculty of Pharmacy, "Iuliu Hațieganu" University of Medicine and Pharmacy, Cluj Napoca

REVIEWERS

Prof. Dr. Paul Mezey, Memorial University of Newfoundland, Newfoundland And Labrador, Canada

Prof. Dr. Luminița Oprean, Faculty of Pharmacy, "Iuliu Hațieganu" University of Medicine and Pharmacy, Cluj-Napoca, Romania

Conf. Dr. Ing. Castelia Cristea - Faculty of Chemistry and Chemical Engineering, "Babeș-Bolyai" University, Cluj-Napoca, Romania.

Date of public defence: **the 27th of November 2012**

Table of Contents

Keywords: sulfite reductase, sulfur monoxyde, DFT, cobalamine, cobinamide, copper bleomycin, thiazole, chalcone, Schiff base

Chapter I

The first chapter provides a brief introduction to heme containing enzymes, of which described are globins (including hydrogen sulfide transporting globins) as well as cytochromes P450 and heme oxygenase.

Cytochromes P450 are enzymes capable of oxidative modifications of both endogenous and exogenous molecules with the purpose of synthesis of useful products and elimination of unwanted compounds. These enzymes are capable of extracting hydrogen atoms even from aliphatic C-H units with a schematic representation of the catalytic cycle given in **Figure I.** The chemical species involved in this process is a radical cation porphyrin bound to a $Fe(IV)O^{2-}$ unit called **Compound I (**see **Figure I.).**

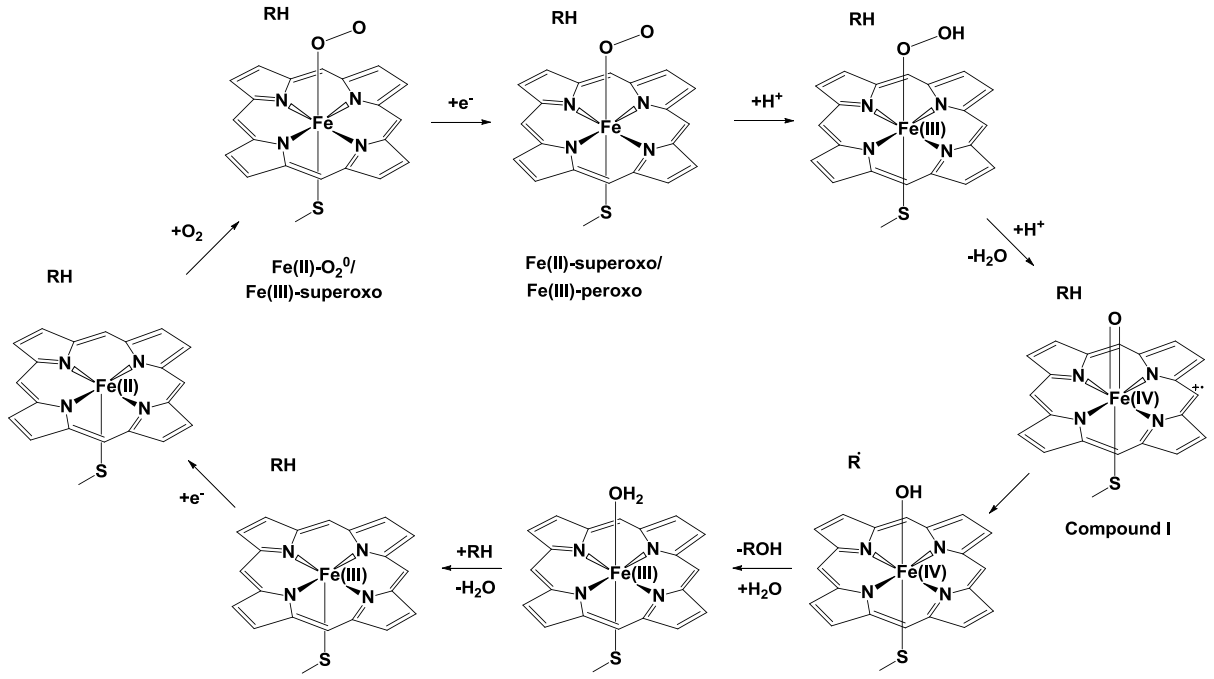

Figure I. Schematic representation of the catalytic cycle of cytP450 derived from ref [1, 2] with the cysteinate axial ligand shown as methylthiolate.

Heme degradation in the human body is performed by the heme oxygenase enzymes, leading to iron, bilirubin and CO. The process occurs through oxygen activation and self oxidation in the *meso* position of the heme (the methylene bridging the pyrrole rings), catalyzed by the heme itself [3]. Further details on heme oxygenase type reactions are given in text. Each relevant section also contains its own introduction.

Chapter II

Chapter II deals with computational studies on the sulfite reductase active site, followed by studies on the interaction on cobalamines and cobinamides with series of different ligands. The last part of the chapter concerns the activation of dioxygen and related species by copper bleomycins.

Section II.1.1.

Sulfite reductase features a siroheme-containing active site and catalyzes the six-electron reduction of sulfite to sulfide at the heme iron [4-8]. A mechanism [9] has been proposed for this process, based on spectroscopic data as well as on the crystal structure of several sulfite reductase adducts [4-8]. After several proton and electron dependent dehydrations, four SO adducts at the iron (with the formal oxidation states of I, II, III and IV) were proposed to be part of the catalytic cycle.

This subchapter deals with the DFT characterization of these adducts with emphasis on the geometric and electronic structures. For this purpose, models were constructed containing iron-porphyrins bound to an axial methylthiolate. Trans to the thiolate, a neutral SO molecule was bound to the iron, both through the oxygen and sulfur atoms. Calculations were performed by using BP86/6-31G**, B3LYP/6-31/G* as implemented in Spartan 06 and M06-L/6-31G** as implemented in Gaussian 09.

One first observation that can be noted is that that the differences between relative energy predictions made by the three functionals examined here – B3LYP, BP86 and M06L, are in some cases rather large – close to 20 kcal/mol – whether concerning the spin state preferences or isomer preferences. This places emphasis on the need to always examine trends between related complexes, as opposed to single values for any given complex in terms of either isomerism or spin state preference.

Another general observation is that although the Fe-OS and Fe-SO isomers are often degenerate in energy, suggesting that they both may be observable, and that interconversion is thermodynamically facile (indeed, calculations performed on Fe(II)-SO models indicate an isomerisation barrier of just over 20kcal/mol); the Fe-SO isomers would be the ones more likely to occur during the catalytic cycle of sulfite reductases – a cycle which is initiated indeed with the sulfite bound to iron via the sulfur, not via the oxygen [4-8].

Of the models employed here the formally Fe(I)-SO/OS states are predicted to be low-spin. The electronic structure in Fe(I)-OS/SO is best described as featuring a superoxide-like SO^- ligand and a porphyrin anion radical, relatively different from the isoelectronic Fe(I)-O_2 states, which at similar levels of theory [10] were previously described as Fe(II)-superoxo, with no porphyrin anion radical. The Fe(II)-SO and Fe(II)-OS adducts are computed to be essentially isoelectronic with Fe(II)-O_2, including the tendency to favor the electromer featuring Fe(III) bound to a superoxide-like SO^-. Concerning the formal Fe(III) models, they were found to feature distinctly weaker bonding to the iron (especially due to the higher-spin preference) than seen in Fe(I)-SO or Fe(II)-SO. No other electromers except Fe(III)-SO^0 electromer are found to contribute significantly to the electronic structure in this case. Fe(IV)-SO models appear to feature the weakest Fe-S bonds of the four oxidation states examined here, with a key factor being the higher-spin state preference. Notably, Fe(IV)-SO is the first of these to occur in the proposed catalytic cycle [9]. The lower-spin states of the Fe(IV)-SO and Fe(IV)-OS appear to feature some unprecedented structures, with the SO ligand attaching either to the nitrogen (with such structures never before observed experimentally [11]) or to the meso carbon in the porphyrin ring as seen in **Figure II**.

Section II.1.2.

The present subchapter deals with the interaction of inorganic sulfides with Compound I type structures as a theoretical probe for the different catalytical route in the last steps of the sulfite reductase. Also, of practical importance is insight into sulfhemes whose mechanism of formation is not completely elucidated and was proposed before to be formed by reaction of hydrogen sulfide with oxygen activated hemes [12-14].

Like in the previous subchapter, models were constructed containing iron(III)-porphyrin bound axially to methylthiolate (for sulfite reductase) and to imidazole (for myoglobin Compound I). Trans to these ligands another series of ligands were bound to the iron center through the oxygen atom (charges given in parentheses): OS (2-), OSH (-), OSH_2 (0) and OHSH (0). Full geometry optimizations were performed using BP86/6-31G** using constrained O-S distances as to mimic dissociation/association along the sulfur and oxygen fragments.

Interesting results can be noted regarding the geometries obtained. Certain models have been observed to give heme oxygenase type reactions during geometry optimization and

comparison with equivalent Fe-O_2 models has been performed in this subchapter. Also, dissociation/association barrier energies, influence of the trans axial ligand (imidazole and methylsulfide) and comparisons with literature electronic structures are given in detail in the full text of the thesis together with a proposed explanation for sulfheme formation and mechanism for sulfite reductase.

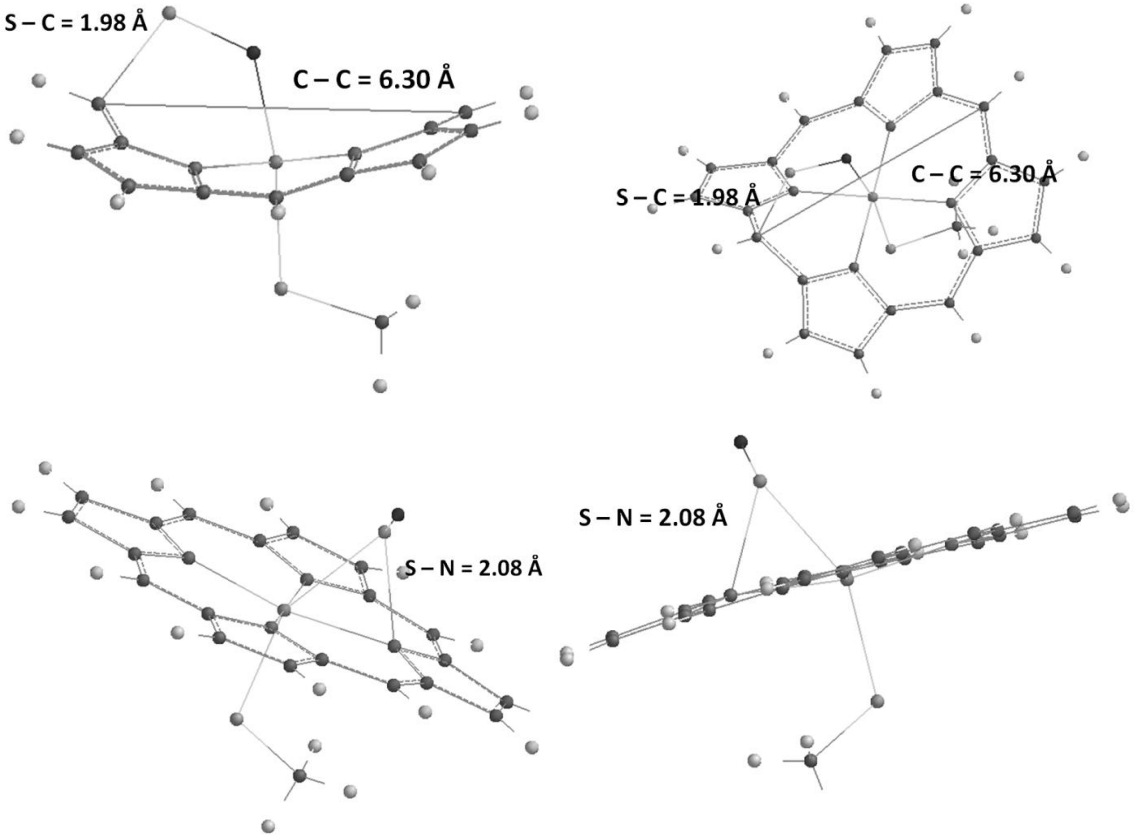

Figure II. Optimized geometries for Fe(IV)-OS singlet (first row, two different views) and for Fe(IV)-SO triplet (second row, two views). Key distances are marked (C-C meso-to-meso for the distorted heme, and S-N for the bridging sulfur geometry).

Section II.1.3.

The present subchapter deals with the last steps of the sulfite reductase pathway, similarly with the previous subchapter, but with emphasis on sulfur bound ligands. The models were constructed by using a formal Fe(III)porphyrin with ligands employed being SO (2-), SOH (-), SOH_2 (0) and SHOH (0) and methylthiolate trans to the ones presented before.

Geometry optimizations were performed with BP86/6-31G** with constrained S-O distances similar to the previous subchapter. The results obtained and comments are presented in detail in the full text of the thesis.

Chapter II.2.

The cobalt-containing corrin macrocyclic compound cobalamin (vitamin B_{12}) is a cofactor for two mammalian enzymes [15, 16]. Redox processes involving cobalamin and its relatives, between Co(III), Co(II) and Co(I), are known to offer opportunities for axial ligand changes reminiscent of those known to dictate reactivity in heme complexes. Axial coordination to the corrin-bound cobalt center depends on the formal oxidation state of the metal ion. As a general rule, the number of axial ligands decrease parallel with the cobalt oxidation state, viz. two axial ligands are bound to the Co(III) center, one axial ligand is bound to the Co(II) center and no axial ligands are bound to the Co(I) center.

This chapter deals with the reactivity of cobalt corrins with different ligands studied by DFT methods and kinetics determined by UV-VIS. For the DFT calculations (BP86 and B3LYP using 6-31G** as basis set), models were constructed containing cobalt (III, II and I) ligated to an unsubstituted corrin macrocyle. Benzimidazole was bound axially so as to mimic the „base-on" forms of cobalamines. Extra sets of axial ligands were employed, of which included are: water, hydroxo, cyanato, methyl, sulfides and thiols, thiocyanate and isothiocyanate, nitrogen oxydes and oxyanions, dioxygen and related species as well as sulfoxylate.

DFT results presented contain geometrical parameters (bond lengths), as well partial charges and spin densities on different subunits of the models (ligand, corrin, cobalt). From the energy point of view, calculated here are binding energies for the ligands (including benzimidazole), proton and electron affinities and comparisons in thermodynamic preference between isomers where applicable.

Each respective subsection contains comparisons with known geometrical parameters from X-ray crystallography [17-25], reaction energies obtained from experiment [26-31] and results obtained by other studies involving DFT [32-36].

As a general conclusion, we have observed that BP86 performs marginally better in describing the geometry of the models when compared to experimentally determined parameters and also the binding affinities. Also, interesting results were obtained in

hexacoordinated formally Co(II) models which are described in the full text. Full details of the experimental procedures are given in the text.

Chapter II.3.

Bleomycin is a drug whose action involves chelating a metal center and then damaging DNA within living cells. A key intermediate in bleomycin's anti-DNA action is a species known as activated bleomycin, ABLM, which, on the basis of spectroscopic and theoretical studies, appears well described as a bleomycin-ferric-hydroperoxo adduct. ABLM's instability has to some extent precluded detailed structural characterization [37-39]. Copper is also known to activate bleomycin and attack DNA in a similar way to (but less much efficiently than) iron-bleomycin [40]. Structural data on Cu-bleomycin is available showing that copper binds in a very similar way to iron [41, 42].

The present chapter deals with a DFT study of dioxygen and related species activation by copper bleomycin using B3LYP with the 6-31G** basis set. The models used are described in the full text, as well as the geometrical parameters, partial charges and spin densities.

Interesting results have been obtained showing that the models studied here behave completely different compared to ferric adducts, both concerning coordination by the bleomycin at the metal center and the electromerism involved, probably providing a different pathway towards DNA damage.

Chapter III.

Thiazoles, chalcones and Schiff bases are important groups present in pharmacologically active compounds [43-55]. Described in this chapter are the synthesis of the thiazole ring using the Hantzsch method followed by the obtaining of several novel compounds: three new thiazole chalcones and four new thiazole Schiff bases. NMR and MS characterization for the obtained compounds as well as the precursors is provided.

References

1. Silaghi-Dumitrescu, R., Cooper, C.E., *Transient species involved in catalytic dioxygen/peroxide activation by hemoproteins: possible involvement of protonated Compound I species.* Dalton Trans., 2005: p. 3477-3482.

2. Meunier, B., S.P. de Visser, and S. Shaik, *Mechanism of oxidation reactions catalyzed by cytochrome p450 enzymes.* Chem Rev, 2004. **104**(9): p. 3947-3980.
3. Kikuchi, G., T. Yoshida, and M. Noguchi, *Heme oxygenase and heme degradation.* Biochemical and Biophysical Research Communications, 2005. **338**(1): p. 558-567.
4. Crane, B.R., L.M. Siegel, and E.D. Getzoff, *Sulfite reductase structure at 1.6 A: evolution and catalysis for reduction of inorganic anions.* Science, 1995. **270**(5233): p. 59-67.
5. Crane, B.R., L.M. Siegel, and E.D. Getzoff, *Probing the catalytic mechanism of sulfite reductase by X-ray crystallography: structures of the Escherichia coli hemoprotein in complex with substrates, inhibitors, intermediates, and products.* Biochemistry, 1997. **36**(40): p. 12120-37.
6. Crane, B.R., L.M. Siegel, and E.D. Getzoff, *Structures of the siroheme- and Fe4S4-containing active center of sulfite reductase in different states of oxidation: heme activation via reduction-gated exogenous ligand exchange.* Biochemistry, 1997. **36**(40): p. 12101-19.
7. Crane, B.R., H. Bellamy, and E.D. Getzoff, *Multiwavelength anomalous diffraction of sulfite reductase hemoprotein: making the most of MAD data.* Acta Crystallogr D Biol Crystallogr, 1997. **53**(Pt 1): p. 8-22.
8. Crane, B.R. and E.D. Getzoff, *The relationship between structure and function for the sulfite reductases.* Curr Opin Struct Biol, 1996. **6**(6): p. 744-56.
9. Silaghi-Dumitrescu, R. and S.V. Makarov, *Siroheme-containing sulfite reductase: a density functional investigation of the mechanism.* Int. J. Quant. Chem., 2012. **112**(3): p. 900-908.
10. Silaghi-Dumitrescu, R. and C.E. Cooper, *Transient species involved in catalytic dioxygen/peroxide activation by hemoproteins: possible involvement of protonated Compound I species.* Dalton Trans., 2005: p. 3477-3482.
11. Silaghi-Dumitrescu, R., *Fe(IV)-Fe(II) electromerism in hemoprotein complexes: implications for ferryl chemistry.* Proc. Rom. Acad. Series B, 2006. **2-3**: p. 95-101.
12. Scharberg, M.A. and G.N. La Mar, *Sulfmyoglobin Derived from Deuterohemin Reconstituted Protein. 2. Molecular and Electronic Structure Determination of Two Extracted Prosthetic Groups.* J. Am. Chem. SOC., 1993. **115**: p. 6522-6528.
13. Chatfield, M.J. and G.N. La Mar, *^{1}H Nuclear Magnetic Resonance Study of the Prosthetic Group in Sulfhemoglobin.* Arch. Biochem. Biophys., 1992. **295**(2): p. 289-296.
14. Chatfield, M.J., G.N. La Mar, and R.J. Kauten, *Proton NMR Characterization of Isomeric Sulfmyoglobins: Preparation, Interconversion, Reactivity Patterns, and Structural Features.* Biochemistry, 1987. **26**: p. 6939-6950.
15. Brown, K.L., *Chemistry and Enzymology of Vitamin B12.* Chemical Reviews, 2005. **105**(6): p. 2075-2150.
16. Dorweiler, J.S., R.G. Finke, and R.G. Matthews, *Cobalamin-Dependent Methionine Synthase: Probing the Role of the Axial Base in Catalysis of Methyl Transfer between Methyltetrahydrofolate and Exogenous Cob(I)alamin or Cob(I)inamide^{+}.* Biochemistry, 2003. **42**(49): p. 14653-14662.
17. Kratky, C., et al., *Accurate Structural Data Demystify B12: High-Resolution Solid-State Structure of Aquocobalamin Perchlorate and Structure Analysis of the Aquocobalamin Ion in Solution.* Journal of the American Chemical Society, 1995. **117**(16): p. 4654-4670.
18. Mebs, S., et al., *Electron Densities of Three B12 Vitamins.* The Journal of Physical Chemistry A, 2009. **113**(29): p. 8366-8378.
19. Randaccio, L., et al., *Similarities and Differences between Cobalamins and Cobaloximes. Accurate Structural Determination of Methylcobalamin and of LiCl- and KCl-Containing Cyanocobalamins by Synchrotron Radiation.* Inorganic Chemistry, 2000. **39**(15): p. 3403-3413.
20. Ouyang, L., et al., *Electronic structure and bonding in hydroxocobalamin.* Spectrochimica Acta Part A: Molecular and Biomolecular Spectroscopy, 2005. **61**(7): p. 1647-1652.
21. Perry, Christopher B., et al., *Probing the Nature of the CoIII Ion in Cobalamins − Spectroscopic and Structural Investigations of the Reactions of Aquacobalamin (Vitamin B12a) with*

Ambident Nucleophiles. European Journal of Inorganic Chemistry, 2003. **2003**(11): p. 2095-2107.
22. Garau, G., et al., *Crystal chemistry and binding of NO2, SCN and SeCN to Co in cobalamins.* Acta Crystallographica Section B, 2003. **59**(1): p. 51-59.
23. Hannibal, L., et al., *Nitroxylcob(III)alamin: Synthesis and X-ray Structural Characterization.* Angewandte Chemie International Edition, 2007. **46**(27): p. 5140-5143.
24. Hassanin, H.A., et al., *Redetermination of the X-ray structure of nitroxylcobalamin: base-on nitroxylcobalamin exhibits a remarkably long Co-N(dimethylbenzimidazole) bond distance.* Dalton Transactions, 2010. **39**(44): p. 10626-10630.
25. Rossi, M., et al., *The structure of a B12 coenzyme: methylcobalamin studies by x-ray and NMR methods.* Journal of the American Chemical Society, 1985. **107**(6): p. 1729-1738.
26. Wolak, M., et al., *Kinetics and mechanism of the reversible binding of nitric oxide to reduced cobalamin B(12r) (Cob(II)alamin).* J Am Chem Soc, 2001. **123**(40): p. 9780-91.
27. Martin, B.D. and R.G. Finke, *Cobalt-carbon homolysis and bond dissociation energy studies of biological alkylcobalamins: methylcobalamin, including a.gtoreq.1015 Co-CH3 homolysis rate enhancement at 25.degree. following one-electron reduction.* Journal of the American Chemical Society, 1990. **112**(6): p. 2419-2420.
28. Martin, B.D. and R.G. Finke, *Methylcobalamin's Full- vs. Half-Strength Cobalt-Carbon sigma Bonds and Bond Dissociation Enthalpies: A>10^15 Co-CH3 Homolysis Rate Enhancement following One-Antibonding-Electron Reduction of Methlycobalamin.* Journal of the American Chemical Society, 1992. **114**(2): p. 585-592.
29. Hung, R.R. and J.J. Grabowski, *Listening to Reactive Intermediates: Application of Photoacoustic Calorimetry to Vitamin B12 Compounds.* Journal of the American Chemical Society, 1999. **121**(6): p. 1359-1364.
30. Joerin, E., A. Schweiger, and H.H. Guenthard, *Single-crystal EPR of the oxygen-17-enriched dioxygen adduct of vitamin B12r: reversible oxygen bonding, electronic and geometric structure and molecular dynamics.* Journal of the American Chemical Society, 1983. **105**(13): p. 4277-4286.
31. Van Doorslaer, S., A. Schweiger, and B. Kräutler, *A Continuous Wave and Pulse EPR and ENDOR Investigation of Oxygenated Co(II) Corrin Complexes.* The Journal of Physical Chemistry B, 2001. **105**(31): p. 7554-7563.
32. Rutkowska-Zbik, D., M. Jaworska, and M. Witko, *Application of the DFT Theory to Study Cobalamin Complexes.* Structural Chemistry, 2004. **15**(5): p. 431-435.
33. Rutkowska-Zbik, D., M. Witko, and G. Stochel, *Ligand binding properties of cobalamins.* Theoretical Chemistry Accounts: Theory, Computation, and Modeling (Theoretica Chimica Acta), 2008. **120**(4): p. 411-419.
34. Selçuki, C., R. van Eldik, and T. Clark, *NO Binding to Cobalamin: Influence of the Metal Oxidation State.* Inorganic Chemistry, 2004. **43**(9): p. 2828-2833.
35. Kuta, J., et al., *Performance of DFT in modeling electronic and structural properties of cobalamins.* Journal of Computational Chemistry, 2006. **27**(12): p. 1429-1437.
36. Jensen, K.P. and U. Ryde, *Theoretical Prediction of the Co−C Bond Strength in Cobalamins.* The Journal of Physical Chemistry A, 2003. **107**(38): p. 7539-7545.
37. Decker, A., et al., *Direct hydrogen-atom abstraction by activated bleomycin: an experimental and computational study.* J Am Chem Soc, 2006. **128**(14): p. 4719-33.
38. Kemsley, J.N., et al., *Spectroscopic studies of the interaction of ferrous bleomycin with DNA.* J Am Chem Soc, 2003. **125**(36): p. 10810-21.
39. Lehnert, N., et al., *Electronic structure and reactivity of low-spin Fe(III)-hydroperoxo complexes: comparison to activated bleomycin.* J Am Chem Soc, 2002. **124**(36): p. 10810-22.
40. Suzuki, T., J. Kuwahara, and Y. Sugiura, *Copper-bleomycin has no significant DNA cleavage activity.* Biochemistry, 1985. **24**(18): p. 4719-21.

41. Sugiyama, M., et al., *The 1.6-A crystal structure of the copper(II)-bound bleomycin complexed with the bleomycin-binding protein from bleomycin-producing Streptomyces verticillus.* J Biol Chem, 2002. **277**(3): p. 2311-20.
42. Danshiitsoodol, N., et al., *The mitomycin C (MMC)-binding protein from MMC-producing microorganisms protects from the lethal effect of bleomycin: crystallographic analysis to elucidate the binding mode of the antibiotic to the protein.* J Mol Biol, 2006. **360**(2): p. 398-408.
43. Block, J. and J.M. Beale, *Wilson and Gisvold's Textbook of Organic Medicinal and Pharmaceutical Chemistry*. Eleventh Edition ed2003: Lippincott Williams and Wilkins. 303-14, 265, 381, 507, 671-2, 721.
44. da Silva, C.M., et al., *Schiff bases: A short review of their antimicrobial activities.* Journal of Advanced Research, 2011. **2**(1): p. 1-8.
45. Kumar, S., D.N. Dhar, and P.N. Saxena, *Applications of metal complexes of Schiff bases-A review.* Journal of Scientific & Industrial Research, 2009. **68**: p. 181-187.
46. Ngameni, B., et al., *Inhibition of MMP-2 secretion from brain tumor cells suggests chemopreventive properties of a furanocoumarin glycoside and of chalcones isolated from the twigs of Dorstenia turbinata.* Phytochemistry, 2006. **67**(23): p. 2573-2579.
47. Wirasathien, L., et al., *Cytotoxic C-benzylated chalcone and other constituents of Ellipeiopsis cherrevensis.* Arch Pharm Res, 2006. **29**(6): p. 497-502.
48. Wei, B.-L., et al., *Synthetic 2',5'-dimethoxychalcones as G2/M arrest-mediated apoptosis-inducing agents and inhibitors of nitric oxide production in rat macrophages.* European Journal of Medicinal Chemistry, 2007. **42**(5): p. 660-668.
49. De Vincenzo, R., et al., *In vitro evaluation of newly developed chalcone analogues in human cancer cells.* Cancer Chemotherapy and Pharmacology, 2000. **46**(4): p. 305-312.
50. Zhang, X.-W., et al., *Synthesis and evaluation of antiinflammatory activity of substituted chalcone derivatives.* Medicinal Chemistry Research, 2010. **19**(4): p. 403-412.
51. Yang, H.-M., et al., *Structural requirement of chalcones for the inhibitory activity of interleukin-5.* Bioorganic & Medicinal Chemistry, 2007. **15**(1): p. 104-111.
52. Simiti, I., et al., *Heterocyclen, 67. Mitt.: Darstellung und Charakterisierung einiger 2-(2-Aryl-thiazol-4-yl)-3-hydroxy-chromone.* Archiv der Pharmazie, 1991. **324**(11): p. 913-915.
53. Awasthi, S., et al., *Potent antimalarial activity of newly synthesized substituted chalcone analogs in vitro.* Medicinal Chemistry Research, 2009. **18**(6): p. 407-420.
54. Jayasinghe, L., et al., *Geranyl chalcone derivatives with antifungal and radical scavenging properties from the leaves of Artocarpus nobilis.* Phytochemistry, 2004. **65**(9): p. 1287-1290.
55. Shukla, P., et al., *Chalcone based aryloxypropanolamines as potential antihyperglycemic agents.* Bioorganic & Medicinal Chemistry Letters, 2007. **17**(3): p. 799-802.